

# RADIAL BASIC FUNCTION-BASED ANALYSIS OF DYNAMIC DEFLECTION OF INVISIBLE FLEXIBLE PAVEMENT LAYER PROFILES

F. C. Yin<sup>1\*</sup> – Y. Zhang<sup>1</sup> – G. C. Zhou<sup>1</sup> – H. Guo<sup>2</sup>

<sup>1</sup>School of Civil Engineering, Harbin Institute of Technology, Harbin 150090, China

<sup>2</sup>SRA, Atlantic City, 08401, USA

## ARTICLE INFO

### Article history:

Received 22.05.2012.

Received in revised form 09.12.2012.

Accepted 17.01.2013.

### Keywords:

Flexible pavement

Layer deflection

Neural network

Radial basic function

Dynamic

## Abstract:

*This study proposes a radial basic function (RBF) neural network model which can simulate the dynamic deflection process of invisible individual layers in the full-scale flexible pavement along with an increase of load repetitions. The training and testing data is formed through empirical and conceptual judgment on the final profiles of the four pavement layers in the test. The independent and dependent variables are defined as the known top and invisible layer deflections respectively. Then, the RBF model produces the numerical results between layer dynamic deflections. Finally, several parameters are suggested to study the response of the invisible pavement layers. The RBF model shows that the implicit dynamic relationship between pavement layer deflections could be modeled by a static state of the flexible pavement. Furthermore, some working features of the pavement might be revealed from its dynamic response.*

## 1 Introduction

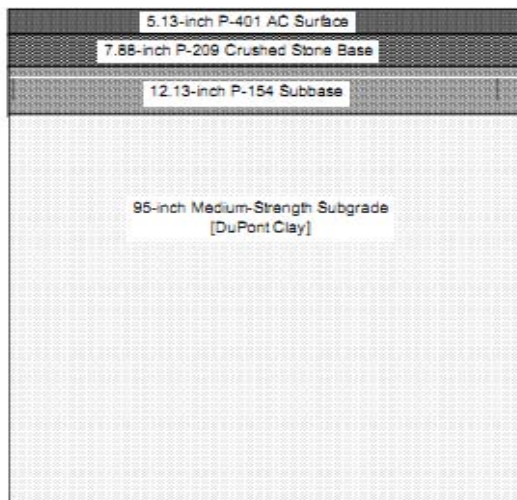
The National Airport Pavement Test Facility (NAPTF), located at the Federal Aviation Administration (FAA) William J. Hughes Technical Center, Atlantic City International Airport, New Jersey, generated a great traffic test of the full-scale flexible medium-strength subgrade (MFC) flexible pavement, in 2001 [1]. Fig. 1a shows the cross-section of the medium-strength subgrade. The test item was trafficked by a six-wheel tridem landing gear configuration on the north side and a four-wheel, dual-tandem landing gear configuration on the south side. After trafficking was completed, a

trench shown in Fig. 1b was dug perpendicular to the centerline of the flexible pavement. The purpose of the trench was to conduct posttraffic investigation into the failure mechanism of the pavement structure; in other words, it was to quantitatively and qualitatively analyze what failure causes result in the defects of the flexible pavement, based on the last deflection state of the pavement layers which could be observed by the trench. Figs. 2a and 2b show the pavement layer profile measurements on the west face and the east face of the trench respectively. The subgrade intrusion into the P-154 base in the six-wheel traffic path and in the four-wheel traffic path is clearly visible in the

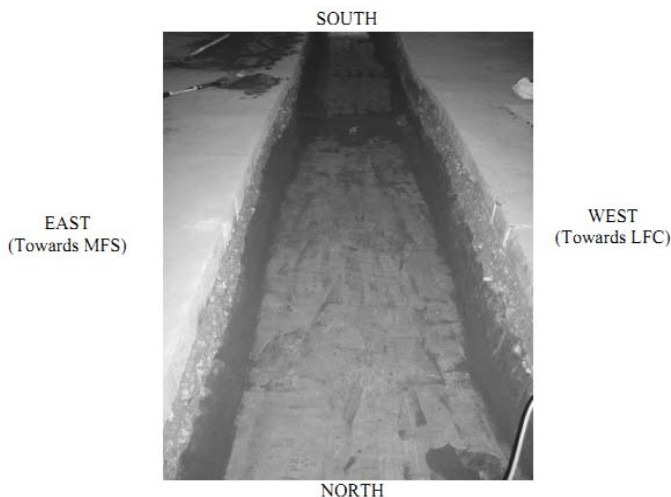
\* Corresponding author. Tel.: +86 132 128 13320;

fax: +86 0451 862 83199

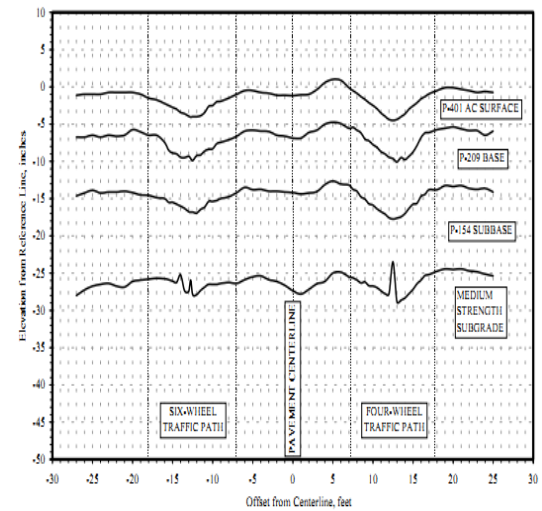
E-mail address: guangchun\_zhou@yahoo.com.cn



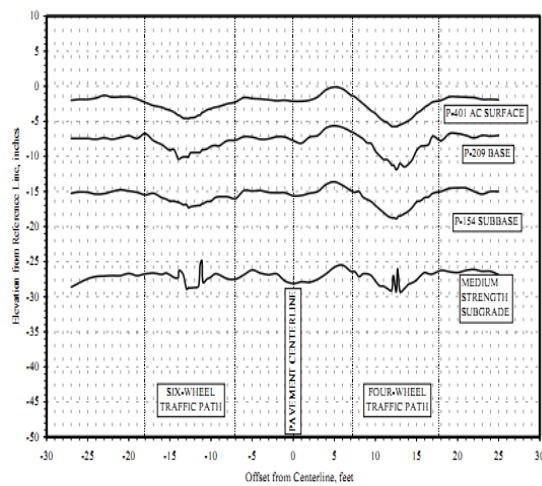
a)



b)



a)



b)

Figure 1. a) The cross-sectional details, and b) dug trench of the pavement.

Figure 2. The pavement layer profile measurements in the trench: a) The west face; b) The east face.

figures. The instrumental data was studied by Donovan and Tutumluer [2]. The conventional finite element analysis (FEA), known as one of the most effective and accurate existing analytical techniques, has been trying to pursue a reliable and accurate prediction of the behavior of the flexible pavement. Kim [3] conducted a wide and detailed FEA of the MFC flexible pavement in his PhD dissertation and gave out some useful conclusions on the behavior and response of the pavement layers. Johnson and Sukumaran [4] used a three-dimensional finite element model to quantify and evaluate the effects of wander and aircraft wheel configurations on the

mechanical response of the pavement layers. However, the FEA models [5-6] are difficult to represent some special appearances at present; for example, the deflections corresponding to the wheel-loading locations for the Medium Strength Subgrade layer conversely develop (bulge) when the load repetitions reach a certain number. Actually, the dynamic behavior of the flexible pavement has highly non-linear relationship with many factors such as loading cases, structural types of pavement layers, material properties, quality of pavement construction, soil moisture and soil temperature. The variation of these factors is great as well, which results in great difficulty in quantifying the effects

of these factors' on the dynamic behavior of the flexible pavement [7].

The difficulty mentioned above indicates: (a) some physical phenomena on flexible pavements might not be simulated by conventional mechanical methods; (b) a static response state for the flexible pavement might include the information enough to model the dynamic response state; (c) some new knowledge might be mined out from the dynamic response of pavement layers.

As indicated by Ceylan and Gopalakrishnan [8], this situation is greatly promising for artificial neural network (ANN) modeling of too complex and highly non-linear problems inherent to flexible pavement. In other words, this case is especially possible to apply the vastly powerful and non-linear interconnections provided in the network architecture that enables an ANN to even model very sophisticated FEA numerical solutions as the state-of-the-art pavement analysis results. They also commented that ANNs have the potential to investigate, properly model and, as a result, better understand some of the complicated pavement working mechanism that has not been well understood and formulated so far.

One of the popular ANNs applied in flexible pavements is back propagation (BP) network such as back-calculation of pavement profiles [9], flexible pavement thickness modeling [10] and pavement modulo back-calculation [11]. However, in the process of training the BP network, all the threshold values and weight values need to be amended, which results in an overall approach to the required accuracy and a relatively slow learning speed. Hence, according to the feature of the issue in this study, the RBF network [12] is applied in consideration of its local approximation and the rapid training speed in amending only a small number of weight and threshold values for each training epoch.

A conceptual judgment seems to suggest that the relationship between the pavement surface deflection and another invisible layer deflection could be reflected through displacements of the individual local points in the layers. It is understood that the RBF model can reflect the dynamic process of the invisible layer deflections, when inputting the deflection values at the points in the surface layer deflection positions in the average intervals. In other words, for the three pavement layers laid under the surface layer, their dynamic deflections

could not be observed during the test, while they become observable or visible through the RBF model proposed in this study.

Then, the analysis of the parameters reflecting the dynamic performance of the flexible pavement can be conducted through the dynamic response process simulated by the RBF model. The analytical results would reveal some features of the pavement layer deflection process.

## 2 Modeling of pavement layer profile

### 2.1 Feature of pavement layer deflection

Four important points are summarized based on the knowledge from the empirical and mechanical realization on the flexible pavement in the past research (the papers except Darken in the references):

- 1) The 3D problem can be simplified as a plain strain problem. In other words, the two profiles of the trench are very similar, which can be verified by comparing Fig. 3a and 3b;
- 2) Individual small local parts in the known surface curve of Layer P-401 have the functional relationship with the corresponding points in the other three layer curves, as shown in Fig. 4 below. The relationship between the layers embodies in not only the last state, but also all the states of the pavement layer deflection development, with the increase of load repetitions;
- 3) Either the deflections of the pavement layers or their relationship is highly non-linear during the working period of the pavement. Actual expression of the non-linear relationship could not be determined at present, but it certainly exists in the measured profiles/data of the pavement layers;
- 4) Since the load repetitions is up to half million, all the points in the individual layer curves could undergo their individual uniformly developing process until the last failure state of the flexible pavement.

### 2.2 The RBF model

The RBF neural network [12] could be suitable for modeling of the pavement layer profile measurements in the trench (West Face) as shown in Fig. 1. The modeling aims at numerically simulating the dynamic process of the pavement layer deflections. According to the special RBF

characteristics in modeling the high non-linear relationship between the variables of a system, the input and output variables are chosen from the measurement of the pavement layer profiles, as shown in Fig. 3. For instance, the functional relation  $R_g$  between the  $i$ th output variable  $g_i$  and the input variables,  $f_{i-1}, f_i$  and  $f_{i+1}$ , as well as the input parameters,  $e_g$  and  $t_g$ , can be stated as Eq. (1):

$$g_i = R_g(f_{i-1}, f_i, f_{i+1}; e_g, t_g) \quad (1)$$

where  $f_{i-1}, f_i$  and  $f_{i+1}$  are three adjacent points in the surface deflection curve of Layer P-401;  $g_i$  is the  $i$ th point in the deflection curve of the layer P-209;  $e_g$  and  $t_g$  are the parameters of the material property and thickness of the layer P-209.

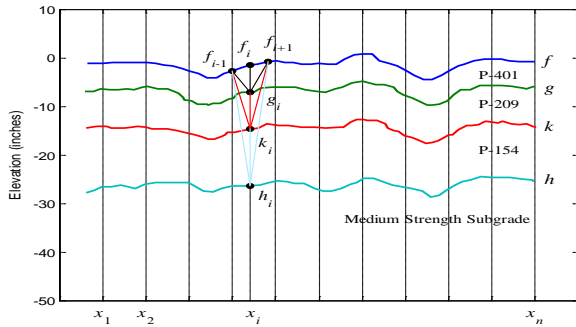


Figure 3. The RBF modeling of the pavement layer profiles.

For the layers P-154 and Medium Strength Subgrade, Eqs. (2) and (3), similar to Eq. (1), can be obtained,

$$k_i = R_k(f_{i-1}, f_i, f_{i+1}; e_k, t_k) \quad (2)$$

$$h_i = R_h(f_{i-1}, f_i, f_{i+1}; e_h, t_h) \quad (3)$$

The position coordinates are set as Eq. (4), along the width of the cross section of the flexible pavement,

$$x_1 < x_2 < \dots < x_i < \dots < x_n \quad (4)$$

For the RBF model, the input variables choose three deflection values,  $f_{i-1}, f_i$  and  $f_{i+1}$ , at the points,  $x_{i-1}, x_i$  and  $x_{i+1}$ , in the surface curve of Layer P-401. The output variable is the deflection value,  $g_i$  or  $k_i$  or  $h_i$ , at one point  $x_i$  in the top curve of Layer P-209 or P-154 or Medium Strength Subgrade.

Thus, a RBF model [12] is established as shown in Fig. 4. The RBF model excludes the parameters and includes the variables corresponding to layer deflections, so the sensibility of this RBF model is only related to the structural parameters such as the node number of the hidden and input layers. A simple verification sets the node number of the hidden and input layers for the RBF model, as listed in Table 1.

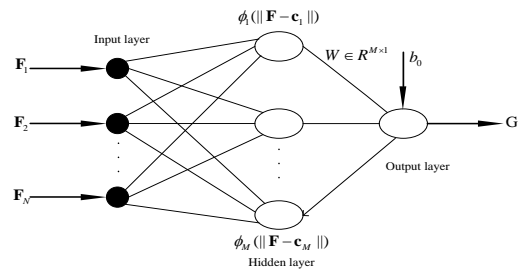


Figure 4. The RBF neural network.

Table 1. The parameters of the RBF model.

RBF model	P-401 → r P-209	P-401 → r P-154	P-401 → Subgrade
Input nodes	3	3	3
Output nodes	1	1	1
Overlap coefficient	200	200	350
Hidden nodes	9	11	12

It should be noted that the analytical correlation between the predicted and tested data in this research project can be not obtained, so the correlation is implicitly expressed by the RBF model.

The training data of the RBF model is set based on the last deflection state of the pavement layers as shown in Fig. 4. The input part in the training data is expressed by the matrix  $\mathbf{F}$ ,

$$\mathbf{F} = \begin{bmatrix} F_1 \\ \vdots \\ F_{i-1} \\ \vdots \\ F_{n-2} \end{bmatrix} = \begin{bmatrix} f_1 & f_2 & f_3 \\ \vdots & \vdots & \vdots \\ f_{i-1} & f_i & f_{i+1} \\ \vdots & \vdots & \vdots \\ f_{n-2} & f_{n-1} & f_n \end{bmatrix}, 1 < i < n-2 \quad (5)$$

The output part in the training is expressed by the vectors corresponding to individual pavement layers,  $\mathbf{G}$ ,  $\mathbf{K}$  and  $\mathbf{H}$ , respectively

$$\mathbf{G} = \begin{bmatrix} g_2 \\ \vdots \\ g_j \\ \vdots \\ g_{n-1} \end{bmatrix}, \quad \mathbf{K} = \begin{bmatrix} k_2 \\ \vdots \\ k_j \\ \vdots \\ k_{n-1} \end{bmatrix}, \quad \mathbf{H} = \begin{bmatrix} h_2 \\ \vdots \\ h_j \\ \vdots \\ h_{n-1} \end{bmatrix}, \quad 2 < j < n-1 \quad (6)$$

### 2.3 The dynamic layer deflections simulated by the RBF model

The RBF model built using the parameters in Table 1 is fully trained using the training data expressed by Eq. (5) and (6). Then, the following scheme is set to simulate the invisible developing process of the top curve of Layer P-209 or P-154 or Medium Strength Subgrade, according to the assumptions (2) and (4).

The training data for the RBF model is empirically taken to cover the key features of layer deflection. Also, due to the limitation of measuring data, the RBF model did not include the parameter of layer thickness. Hence, the 50 known deflection values  $f(x_i)$  of the pavement surface layer P-401 in Fig. 3, corresponding to 50 coordinates,  $x_1 < x_2 < \dots < x_i < \dots < x_n$ , along the width of the pavement, are treated as the input data of the RBF simulation. For a deflection  $f(x_i)$ , it is divided into the 50 average interval values, as shown by Eq. (7)

$$0, \frac{1}{50} f(x_i), \frac{2}{50} f(x_i), \dots, \frac{49}{50} f(x_i), f(x_i); i=1,2,\dots,50 \quad (7)$$

Thus, the 50 developing stages of the surface curve  $f(x)$  of Layer P-401 are described as the 50 groups of input data, as shown by Eq. (8) and Fig. 5

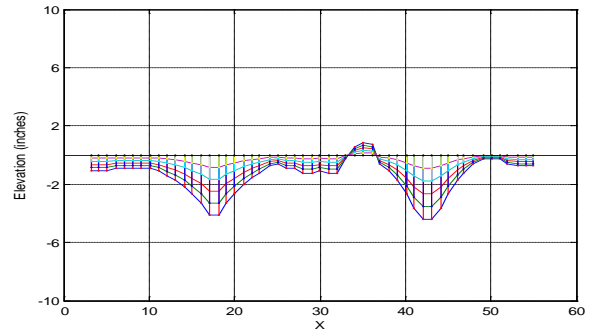


Figure 5. The discrete dynamic process of the surface deflection curve of Layer P-401.

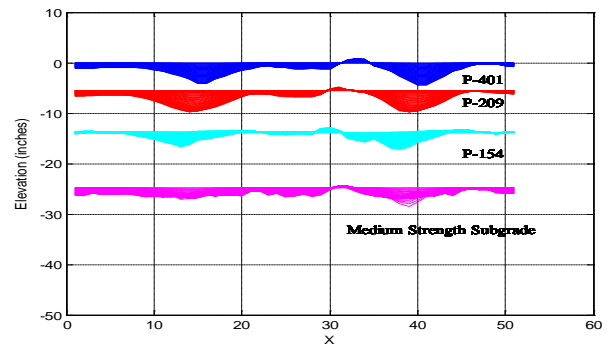


Figure 6. The dynamic process of the layer deflections simulated by the RBF model.

$$\begin{aligned} &0, 0, \dots, 0 \\ &\frac{1}{50} f(x_1), \frac{1}{50} f(x_2), \dots, \frac{1}{50} f(x_{50}) \\ &\frac{2}{50} f(x_1), \frac{2}{50} f(x_2), \dots, \frac{2}{50} f(x_{50}) \\ &\dots \\ &\frac{49}{50} f(x_1), \frac{49}{50} f(x_2), \dots, \frac{49}{50} f(x_{50}) \\ &f(x_1), f(x_2), \dots, f(x_{50}) \end{aligned} \quad (8)$$

After inputting the data in Eq. (8) into the trained RBF model group by group, the dynamic top curves of Layers P-209, P-154 and Medium Strength Subgrade are obtained as shown in Fig. 6.

### 3 Verification of the dynamic simulation result

#### 3.1 Comparison of RBF simulation with testing result

From Fig. 6 whose dynamic picture has been programmed, the invisible dynamic process of the

curves simulated by the RBF model basically reflects the four working features in the real test of the flexible pavement:

- 1) The largest deflection positions in the individual layers correspond to the wheel-loading positions;
- 2) For each layer, the bulge phenomenon occurs at the region between two wheel-loading positions, because of the extrusion from the neighboring regions vertically corresponding to the wheel-loading positions;
- 3) Before the subgrade reaches about 60% of the total settlement of the pavement surface layer, the bottom layer (Medium Strength Subgrade) deflection close to the largest deflection position develops greater than the other layers;
- 4) After the subgrade reaches about 60% of the total settlement of the surface layer, the bottom layer (Medium Strength Subgrade) develops conversely (bulge) at two locations vertically corresponding to the wheel-loading positions, and the deflection development of the other layers still keeps in the first direction. This phenomenon is quite difficult to simulate through the existing FEA techniques. Hence, it could be remarked that the proposed RBF model could simulate the dynamic process of the invisible layer curves of the flexible pavement well. In other words, the whole deflection process of the pavement layers could be reflected by a RBF model, based on only a deflection state of the flexible pavement.

### 3.2 Comparison between the RBF, FEA and testing results

#### (1) FEA models.

Two FEA numerical simulations of the pavement response are conducted by the 2D and 3D FEA models shown in Fig. 7. The geometrical and material parameters of the pavement used in the FEA models are given in Table 2. Boundary conditions of both FEA models are the fixed bottom edge, simply supported vertical edges and free top surface. Load is the uniformly distributed tire pressure 1.303MPa within the cycle area (radius = 152.4mm). The 2D FEA model of the pavement is built as 3048mm in width and 3051mm in depth. The 3D FEA model of the pavement is built as 8890mm in length, 8890mm in width and 3051mm in depth. The loading rate and time are 8km/h and 4s. The FEA simulation is in the range of elasticity.

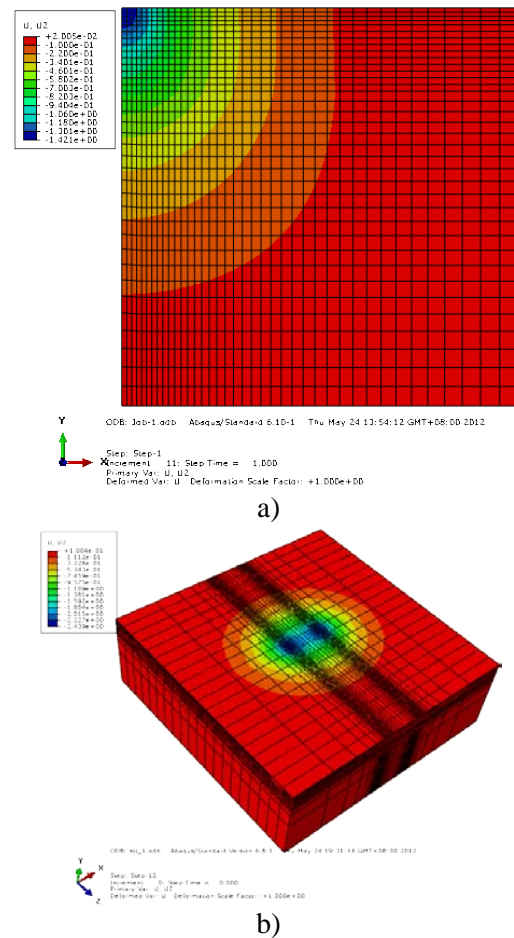


Figure 7. Contour plots of pavement layer deflection calculated by the FEA program: a) The axially symmetrical 2D FEA model; b) The 3D FEA model.

Table 2. Geometrical and material parameters for FEA simulator.

Layer	Thickness (mm)	Poisson's Ratio	Elastic Modulus (MPa)
P-401	130	0.35	2759
P-209	200	0.38	207
P-154	308	0.38	138
Subgrade	2413	0.40	41

The FEA program Abaqus is used in the numerical simulation.

#### (2) Comparison between the RBF, FEA and testing results

Figs. 8 and 9 show the displacements of points in Layers P-401 and P-209 calculated by the 2D and

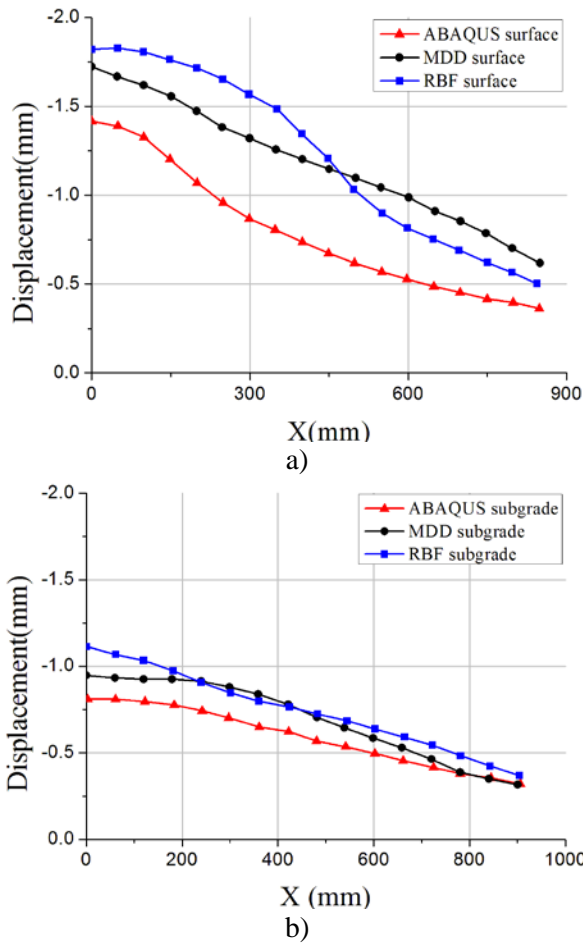


Figure 8. Displacements of points in Layers P-401 and P-209 (2D FEA model): a) Layer P-401; b) Layer P-209.

Table 3. Comparison between the RBF, FEA (2D, 3D) and MDD results for Layers P-401 AC and Subgrad.

Parameter	Layer	RBF & testing results	FEA(2D) & testing results	FEA(3D) & testing results
Average Error of Deflection	P-401	0.1460	0.3580	0.3103
	Subgrade	0.0940	0.1229	0.2265

3D FEA models and the RBF model, as well as the corresponding displacements measured in the test. Table 3 gives out the average errors between the testing result and the RBF or FEA (2D and 3D models) results, for Layers P-401 and Subgrade. The comparison indicates that the RBF model can simulate the deflections of Layers P-401 and Subgrade closer to the testing results than ones from the FEA results.

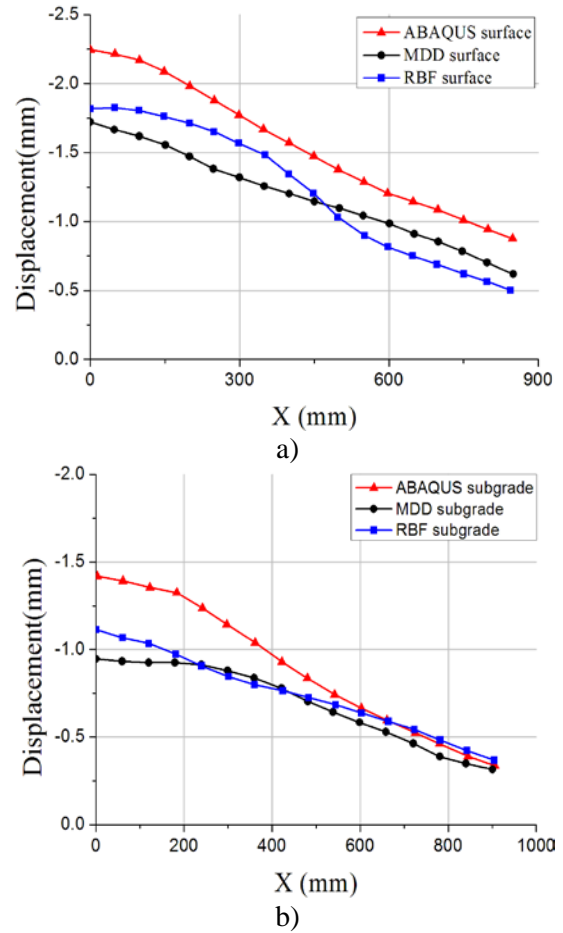


Figure 9. Displacements of points in Layers P-401 and P-209 (3D FEA model): a) Layer P-401; b) Layer P-209.

#### 4 Investigation into dynamic change of layer thickness and deflection

The dynamic layer deflections predicted by the RBF model could be utilized to conduct the investigation into the dynamic behavior of the flexible pavement. Several parameters below are proposed to describe the dynamic features of the flexible pavement.

##### 4.1 Investigation into the relationship between the deflection capacity and average thickness change of the layer

The ratio,  $\psi_{average,l}(j)$  shown in Eq. (9), is set to analyze the relationship between the average deflection capacity and the average thickness change of the  $l$ th layer in the  $j$ th stage

$$\psi_{average,l}(j) = \frac{D_{average,l}(j)}{t_{average,l}(j)}, \quad l \text{ is the layer number, } l=1,2,3 \quad (9)$$

where  $D_{average,l}(j)$  is the average deflection capacity of the  $l$ th layer in the  $j$ th stage, which is calculated by Eq. (10)

$$D_{average,l}(j) = \frac{1}{n} \sum_{i=1}^n d_{l,i}(j) \quad (10)$$

where  $d_{l,i}(j)$  is the deflection value of Point  $i$  in the  $l$ th top curve in the  $j$ th stage;  $t_{average,l}(j)$  is the average thickness of the  $l$ th layer in the  $j$ th stage, which is calculated by Eq. (11)

$$t_{average,l}(j) = \frac{1}{n} \sum_{i=1}^n \left| |d_{l,i}(j)| - |d_{l+1,i}(j)| \right| \quad (11)$$

where  $\left| |d_{l,i}(j)| - |d_{l+1,i}(j)| \right|$  is the thickness value of Point  $i$  in the  $l$ th layer in the  $j$ th stage.

Similarly,  $\psi_{max,l}(j)$  shown in Eq. (12) is set to analyze the relationship between the maximum deflection value and the average thickness change of the  $l$ th layer in the  $j$ th stage  $j$ , that is,

$$\psi_{max,l}(j) = \frac{D_{max,l}(j)}{t_{average,l}(j)} \quad (12)$$

where  $D_{max,l}(j)$  is the maximum deflection of the  $l$ th layer in the  $j$ th stage, which is chosen by Eq. (13)

$$D_{max,l}(j) = \max_{i=1}^n [d_i(j)] \quad (13)$$

Here, it should be noted that the 1<sup>st</sup> layer is P-401 AC surface, the 2<sup>nd</sup> layer is P-209 Base and 3<sup>rd</sup> layer is P-154 Subgrade.

In Figs. 10-12, the  $\psi_{average,l}(j)$  and  $\psi_{max,l}(j)$  curves are plotted based on the dynamic process of the invisible layer deflections of the flexible pavement simulated by the proposed RBF model.

These  $\psi_{average,l}(j)$  and  $\psi_{max,l}(j)$  curves indicate:

1) Basically, no matter how much the average thickness change of the 1st and 2nd layers is, the corresponding layer deflection capacity keeps

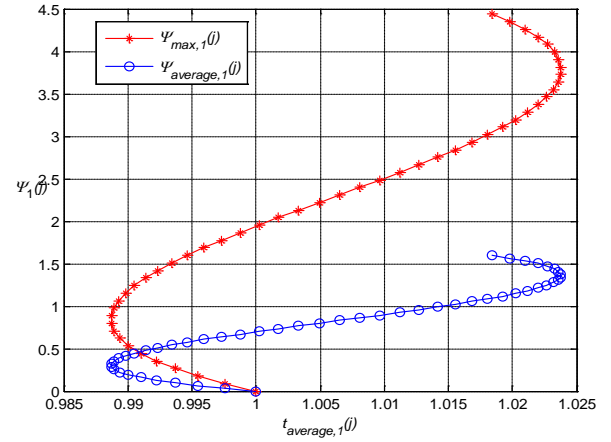


Figure 10. The curve of  $\psi_1(j)$ .

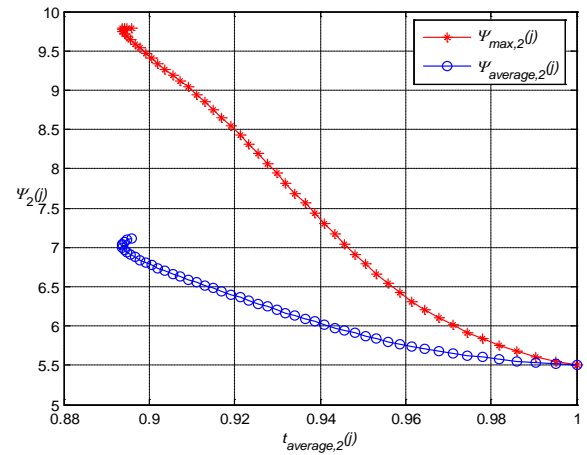


Figure 11. The curve of  $\psi_2(j)$ .

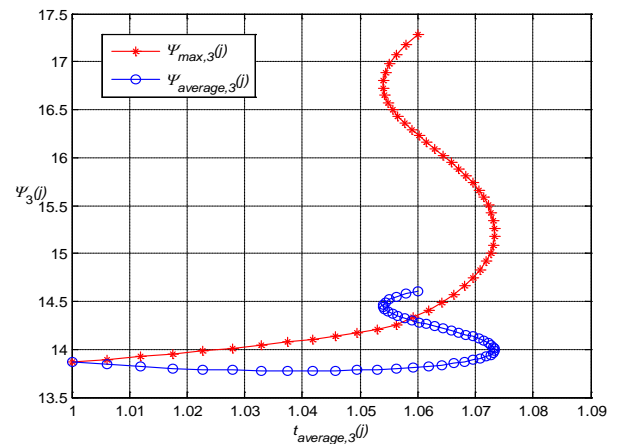


Figure 12. The curve of  $\psi_3(j)$ .

increasing approximately linearly. In other words, the layer deflection capacity develops faster than the corresponding average thickness change of the 1st and 2nd layers;

2) However, for the 3rd layer, its layer deflection capacity and corresponding average thickness change develops in the same amplitude within about 50% of the final deflection of the P-401 AC Surface. Then, the layer deflection capacity develops faster than the corresponding average thickness change. Particularly, the maximum deflection of the 3rd layer develops in larger amplitude than the corresponding maximum deflections of the 1st and 2nd layers, because the breaking of the top of the 3rd layer at the positions is vertical to the loading positions.

The phenomenon mentioned above seemingly implies that the deflection capacity of the layer is more important than the thickness change of the pavement layer. Therefore, more attention should be paid to the deflection capacity of the pavement layer, in the analysis of the response and behavior of the flexible pavement, even in the design and monitoring of the flexible pavement.

**4.2 Investigation into the relationship between the maximum deflection values of two layers**

Fig. 13 plots three ratios,  $\sigma_{\max,12}(j)$ ,  $\sigma_{\max,13}(j)$  and  $\sigma_{\max,23}(j)$ , between the maximum deflection values of any two layers in the  $j$ th stage. The corresponding calculation equations (16) are given below

$$\sigma_{\max,12}(j) = \frac{d_{\max,1}(j)}{d_{\max,2}(j)}, \sigma_{\max,13}(j) = \frac{d_{\max,1}(j)}{d_{\max,3}(j)}, \sigma_{\max,23}(j) = \frac{d_{\max,2}(j)}{d_{\max,3}(j)} \tag{16}$$

From Fig. 13, the investigation can be conducted into the relationship between the maximum deflection values of any two among the three layers in the individual stages.

1) For the curves,  $\sigma_{\max,13}(j)$  and  $\sigma_{\max,23}(j)$ , the maximum deflection in the 3rd layer suddenly increases in a much larger amplitude than the 1st and 2nd layers, after about 26% of the final deflection of the P-401 AC Surface. This might be because a local instability of the 3rd layer at the

position where the maximum deflection occurs when the compressive force and its acting duration reach a certain state. Empirically, the 3rd layer

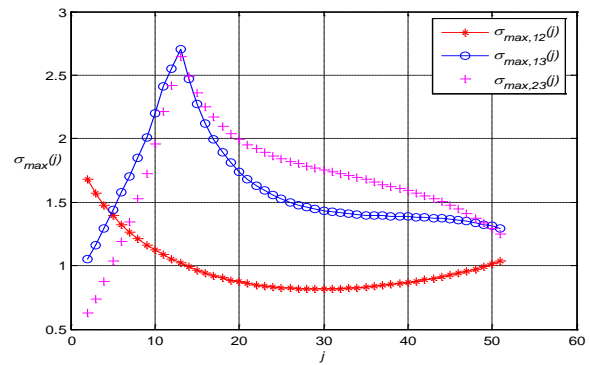


Figure 13. The curves of the ratios between the maximum deflection values of any two layers.

might be built in a relatively low engineering or material quality, which results in this instability of the layer;

2) For the curve  $\sigma_{\max,12}(j)$ , the ratio between the maximum deflection values of the 1st and 2nd layers keeps relatively stable without a phenomenon of instability, which could be due to that these two layers were built in a higher engineering or material quality than the 3rd layer.

In total, the analysis shows some dynamic features of the working performance of the pavement layers, which cannot be obtained without a dynamic response process of the pavement layers. Consequently, some behaviors of the flexible pavement relating to the dynamic response process could be revealed by analytical techniques such as statistical techniques, modeling output techniques.

**5 Conclusions**

This study develops a RBF neural network application in simulating the dynamic deflection process of the invisible layer profile of the flexible pavement. The proposed RBF model is validated through the FEA and testing data. Therefore, it could be stated as follows:

1) The RB model truly simulates the dynamic deflection process of the pavement layers, based on only one last deflection state of the pavement layer profile. It reflects the dynamic deflection features of the layer profile observed at FAA’s NAPTF, in

which some of the response appearance could be difficult to reveal using the existing conventional methods;

2) The RBF model can directly make use of the testing data in the RBF modeling without a mechanical assumption in the conventional methods;

3) Subsequently, according to the result simulated by the RBF model, the dynamic behavior of the flexible pavement can be analyzed to reveal some knowledge unseen in the test and the existing numerical simulations.

The analytical results could be referred to the further research on the flexible pavement high non-linear problems and the application of the testing data in a non-transitional way.

### Acknowledgments

The authors would like to thank for the financial sponsorship of the Youth Foundation of Education Department of Sichuan Province (No. 10ZB010), China. Thanks are extended to the financial support from the Yoh Foundation, USA. Also, thanks for Miss Tiantian Sun's contribution in the FEA simulation.

### References

- [1] Navneet G, et. al.: *Report: Posttraffic Testing at the National Airport Pavement Test Facility: Test Item MFC*, U.S. Department of Transportation, Federal Aviation Administration, 2001.
- [2] Donovan, D., Tutumluer, E.: *Analysis of NAPTF Trafficking Response Data for Pavement Foundation Deformation Behavior*, In Proceedings of FAA Worldwide Airport Technology Transfer Conference, Atlantic City, USA, 2007.
- [3] Kim, M.: *Three-Dimensional Finite Element Analysis of Flexible Pavements Considering Nonlinear Pavement Foundation Behavior*, PhD Dissertation, University of Illinois at Urbana-Champaign, 2007.
- [4] Johnson, D. and Sukumaran B.: *Investigation of the Performance of Flexible Airport Pavements under Moving Aircraft Wheel Loads with Wander Using Finite Element Analysis*, Proceedings of GeoHunan International Conference, Challenges and Recent Advances in Pavement Technologies and Transportation Geotechnics, Changsha, Hunan, China, 2009, 44-49.
- [5] Wang, J.: *Three-Dimensional Finite Element Analysis of Flexible Pavement*, Master Thesis, University of Maine, ME, 2001.
- [6] Saad, B., Mitri, H., Poorooshash, H.: *Three-Dimensional Dynamic Analysis of Flexible Conventional Pavement Foundation*, Journal of Transportation Engineering, 131 (2005), 6, 460-467.
- [7] Mun, S.: *Nonlinear finite element analysis of pavements and its application to performance evaluation*, PhD Thesis, Department of Civil Engineering, North Carolina State University 2003.
- [8] Ceylan H., Gopalakrishnan K.: *Artificial neural network models incorporating unbound material nonlinearity for rapid prediction of critical pavement responses and layer moduli*, Intelligent and Soft Computing in Infrastructure Systems Engineering, Springer, 2009.
- [9] Gucunski, N., Krstic, V.: *Backcalculation of pavement profiles from spectral-analysis-of-surface-waves test by neural networks using individual receiver spacing approach*, Transportation Research Record, 1526 (1996), 2, 6-13.
- [10] Saltan, M., Tigdemir, M., Karasahin, M.: *Artificial Neural Network Application for Flexible Pavement Thickness Modeling*, Turkish Journal of Engineering and Environmental Sciences, 26 (2002), 3, 243-248.
- [11] Gopalakrishnan, K.: *Neural Network-Swarm Intelligence Hybrid Nonlinear Optimization Algorithm for Pavement Moduli Back-Calculation*, Journal of Transportation Engineering, 136 (2010), 6, 528-536.
- [12] Darken, C. J., Moody, J.: *Fast learning in networks of locally-tuned processing units*, Journal of Neural Computation, 1 (1989), 2, 281-294.